Electrical impedance tomography to monitor unsaturated moisture flows, and to detect corrosive elements and cracking in cementitious materials

Aku SEPPÄNEN [1], Milad HALLAJI[2], Danny SMYL[2], Mohammad POUR-GHAZ[2]

[1] Department of Applied Physics, University of Eastern Finland, Kuopio, FINLAND
Aku.Seppanen@uef.fi
[2] Department of Civil Construction and Environmental Engineering, North Carolina State University, Raleigh, NC 27695, USA mpourghaz@ncsu.edu

Key words: Other Methods, concrete, condition monitoring, electrical methods, damage detection, electrical impedance tomography, corrosion, imaging.

Abstract
Electrical impedance tomography (EIT) is an imaging modality which uses electrical measurements to reconstruct two- or three-dimensional (2D/3D) electrical conductivity distributions in target objects. In this paper, we discuss two recent applications of EIT in structural health monitoring. First, we study the feasibility of EIT for imaging unsaturated moisture flows in cement-based materials. In the experiments, specimens are monitored with EIT during the water ingress in the specimens. The results indicate that EIT is able to detect the moisture movement and to show approximately the shape and position of the water front. Secondly, we develop EIT -based surface sensing systems, or sensing skin, for detecting and localizing the ingress of chlorides and cracking – two phenomena which are of concern in many structures, including reinforced concrete structures. In the experiments, the sensing skins are tested using concrete substrates. The results demonstrate the feasibility of a single-layer sensing skin for detecting cracks, and further, show the potential of a multi-functional multi-layer sensing skin for simultaneously detecting corrosive elements and cracks, and for distinguishing between them.

1 INTRODUCTION

The durability of reinforced concrete structures is related to the ability of concrete to impede the ingress of water and aggressive agents, as the presence of ions accelerate the corrosion of the steel reinforcement, leading to the decrease of the service life of the concrete structure [1]. One of the main contributing factors to the concrete durability is thus cracking: Although the presence of cracks in concrete does not necessarily imply structural deficiency, cracks may provide preferential flow paths for water and aggressive agents to enter the concrete.

Several advanced methods exist for monitoring moisture movement [2, 3, 4], but many of these methods are invasive, expensive to apply and are mainly limited to laboratory due to the required facilities. Electrically based methods [5, 6], on the other hand, are often noninvasive, inexpensive and rapidly performed.

Conventional electrical techniques, such as impedance spectroscopy use measurements between pairs of electrodes embedded in concrete and/or attached on its surface. Such measurements, however, provide only very limited information on the distribution of moisture in concrete. An imaging modality that uses electrical surface measurements to reconstruct the distribution of the electrical conductivity is referred to as electrical impedance tomography (EIT). Recently, EIT has been shown to provide information on 1D [7], 2D [8] and 3D [9] moisture flows in concrete. In Section 3, the findings of paper [8] are briefly reviewed.

Electrical methods have also been applied for detection of cracks. Especially, one recently developed approach to crack detection is the use of electrically conductive surface mounted sensors. These sensors are made of electrically conductive materials (e.g., thin metal foils, or copper- or silver-based paints) that are applied to the surface of the structure. When the concrete substrate is strained, the sensor is stretched and its electrical resistance increases slightly. If the surface of the substrate cracks, the sensor ruptures and its resistance increases by orders of magnitude. Therefore, by monitoring the resistance of the sensor, cracking of the substrate can be detected. Conductive surface sensors have been recently developed for crack detection in both 1D and 2D settings. While 1D sensors, usually made of strips of conductive materials [10, 11], can indicate the presence of a crack, the 2D sensors can be used locate cracks and even reveal their shapes [12,13, 14, 15, 16]. These 2D sensors were based on EIT imaging of a (single-layer of) conductive material attached/painted on the substrate surface, see Section 4. In Section 5 (and in the related manuscript [17]), we study whether the functionality of the EIT-based sensing skin could be extended to detect the presence of chloride ions. For this aim, we construct a double-layer sensing skin, where one layer is sensitive to both cracking and chlorides and the second layer is sensitive to cracks only.

2 ELECTRICAL IMPEDANCE TOMOGRAPHY

In electrical impedance tomography (EIT), objects are imaged based on electrical measurements from the object surface. A set of electric currents are injected into the object through electrodes attached on the surface, and corresponding to each current injection, electric potentials on the electrodes are measured. Based on the resulting set of (indirect) measurements, the spatial distribution of the electrical conductivity within the object is reconstructed. The method is schematically illustrated in Figure 1. EIT has various applications in, e.g., geophysical exploration [18], biomedical imaging [19], industrial process monitoring and control [20]. For a review on EIT, see e.g. [21].

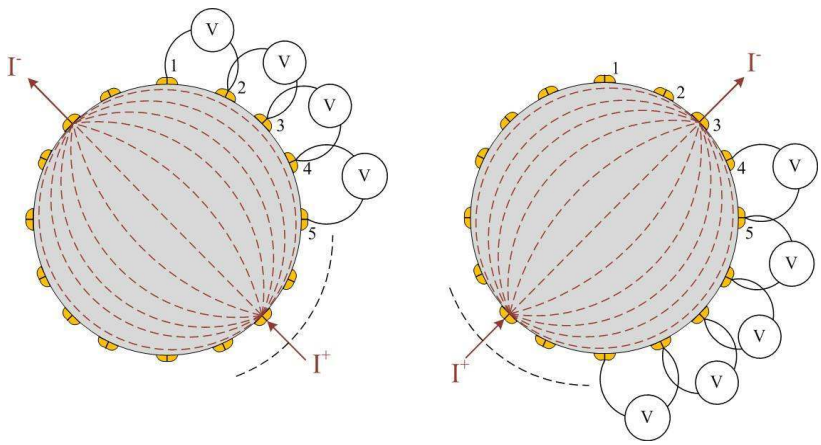

Figure 1: Schematic illustration of EIT measurements corresponding to two current injections.

In this paper, EIT is used in two distinct setups aiming at structural health monitoring of cement-based materials: 1) Imaging of unsaturated moisture flow in concrete. Here, electrodes are attached on concrete surface, and the aim is to monitor the flow based on the reconstructed change of the electrical conductivity of the cement-based material (Section 3). 2) Detection of cracks (Section 4) or chlorides and cracks (Section 5) on the surface of concrete using an EIT-based sensing skin. Thus, while the first setup aims at reconstructing the distributed conductivity within the cement-based material itself, in the second setup the phenomena on the concrete surface are inferred via reconstructing the electrical conductivity of paint layer(s) applied on the concrete surface.

It is worth noticing that the image reconstruction problem of EIT (i.e., computing the 2D/3D conductivity distribution based on boundary potential measurements) is mathematically an ill-posed inverse problem, and special methods for the solutions are needed. For the computational methods used in this paper, we refer to works [8, 15].

3 IMAGING OF MOISTURE FLOW USING EIT

3.1 Experiments

The objective of this study was to investigate whether EIT could give feasible information on the distribution of moisture in cement-based materials. In this experimental study, the results of EIT were corroborated with high resolution neutron radiography.

Figure 2 shows a photograph of a cuboid-shaped specimen (dimensions 7.6 cm × 7.1 cm × 1.37 cm) used in the experiment. A water reservoir covering the entire top surface was mounted on top of the specimen. For EIT measurements, 15 electrodes were attached on the perimeter of the specimen. The electrodes were made by applying a thin layer of colloidal silver paint directly to the surface of the cement paste, and then applying a layer of conductive silver-filled epoxy on top of the silver paint. EIT and neutron radiography measurements were simultaneously carried out during water ingress. The photograph in Figure 2 was taken 60 min after the addition of water; the dark surface area indicates the wetted region. For details of the experiment, we refer to [8].

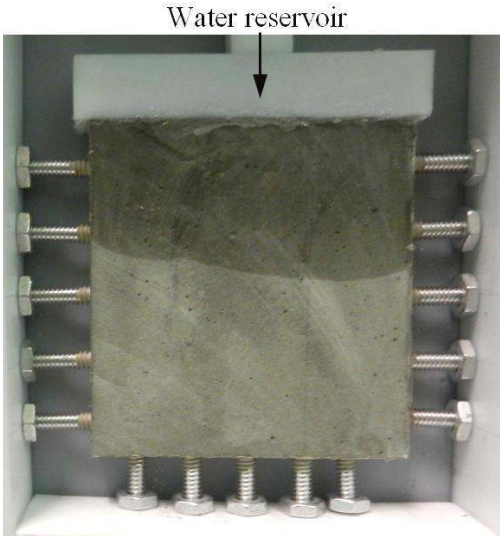

Figure 2: Imaging of moisture flow with EIT. Photograph of the specimen 60 minutes after adding water.

3.2 Results

The results of the moisture flow monitoring experiment are shown in Figure 3. The left column illustrates the change of the water content, w, with respect to the initial state. These images were calculated from the neutron radiographs as described in [8]. The right column shows the reconstructed change of the electrical conductivity, $\Delta\sigma$, with respect to the initial state.

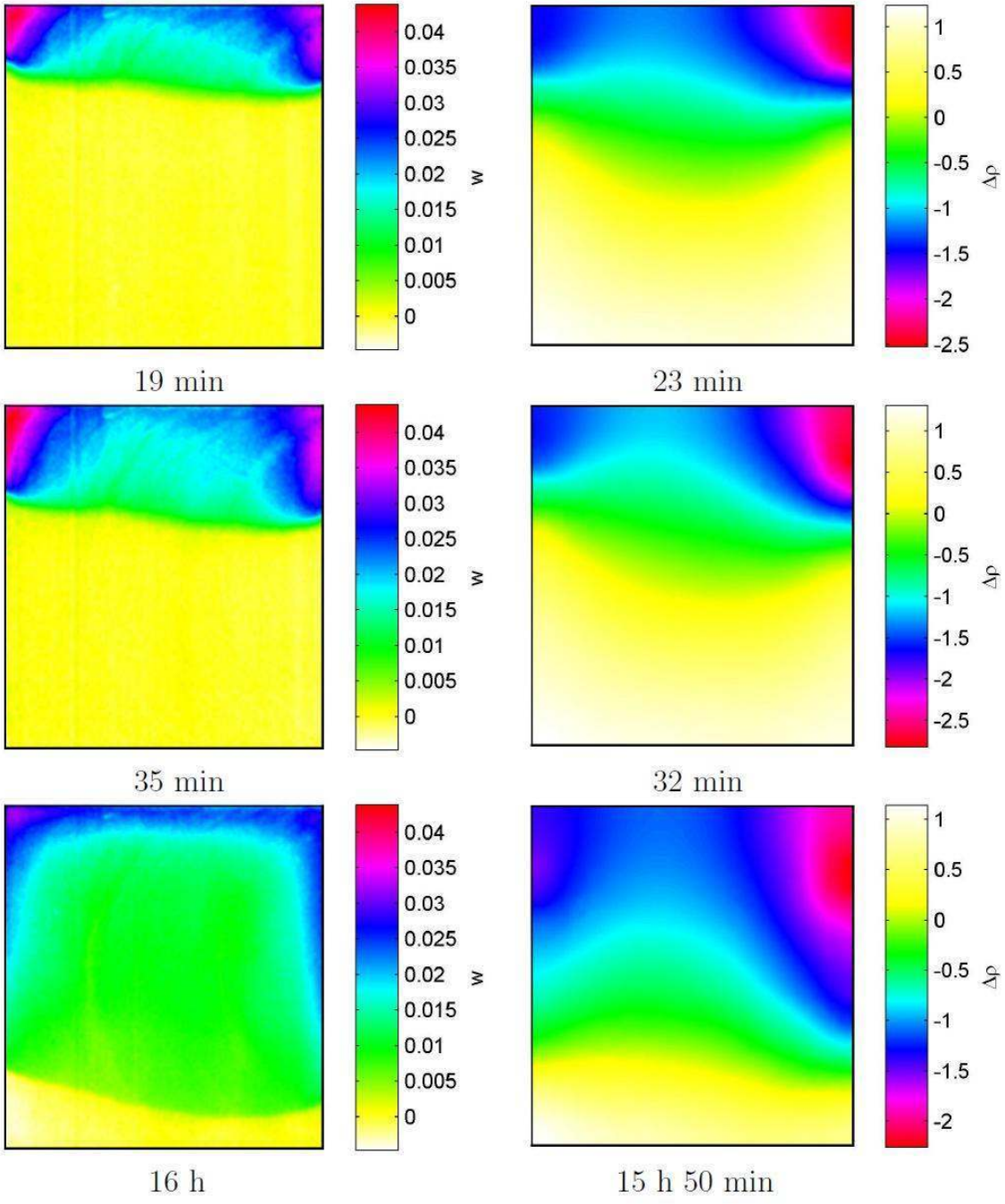

Figure 3: Imaging of moisture flow; neutron radiography images (left column) and EIT reconstructions (right column). The times of the neutron exposures/ERT measurements are shown under the images.

The dependence between the water content and the electrical conductivity is non-linear, and hence, the two columns in Figure 3 can only be compared qualitatively. It is also worth noticing that the times of the neutron exposures and the EIT measurements are not equal, and that the color scales of the images have been deliberately chosen to highlight the similarities of the neutron radiographs and the EIT reconstructions. Nevertheless, the qualitative comparison between the two sets of images in Figure 3 clearly demonstrate the feasibility of EIT for monitoring the moisture flow in 2D. Indeed, the EIT images show at least approximately the evolution of the moisture front, reveal faster flow rate in the right half of the specimen, and reveal that the moisture content is highest in the top corners of the specimen. For further discussion, see [8].

4 CRACK DETECTION USING EIT-BASED (SINGLE-LAYER) SENSING SKIN

4.1 Experiments

In the second experiment, the application of a painted EIT-based sensing skin for detection of cracks in concrete was studied. The sensing skin was made of electrically conductive copper paint applied on the surface of a reinforced and notched concrete beam. The beam was then 4-point bended to induce a crack pattern on the surface where the sensing skin was applied. For EIT measurements, 32 electrodes were placed in the perimeter of the sensing skin. The details of the experiment are given in [15].

4.2 Results

The results of the experiment are shown in Figure 4. The left column of the figure shows photographs of the sensing skin at six states of loading: 0 kN, 18.2 kN, 29.8 kN, 39.1 kN, 71.2 kN and 85.0 kN. As a consequence of loading, an evolution of a crack pattern on the sensing skin was observed. In the photographs, the cracks are highlighted in red.

The reconstructed 2D conductivity distributions within the sensing skin clearly reveal the cracking of the substrate surface (featuring $\sigma = 0$ indicated by red at least roughly in all locations of cracks). Although at some instants of time, the dimensions of the cracks are not correct and/or the conductivity in the location of the crack is above 0 (see, e.g. lines 2-4 in Figure 4), the resolution of the sensing skin is surprisingly high, taking into account that EIT is usually considered as a low resolution imaging modality due to the diffusive nature of the propagation of the electric current. The relatively high accuracy of the EIT images is based on the novel computational methods introduced in [15]. It is worth noticing, that the resolution of the images in Figure 4 is higher than [15]; this was achieved by using denser finite element meshes in the discretization of the associated mathematical model; for more information on the effect of discretization, we refer to [16].

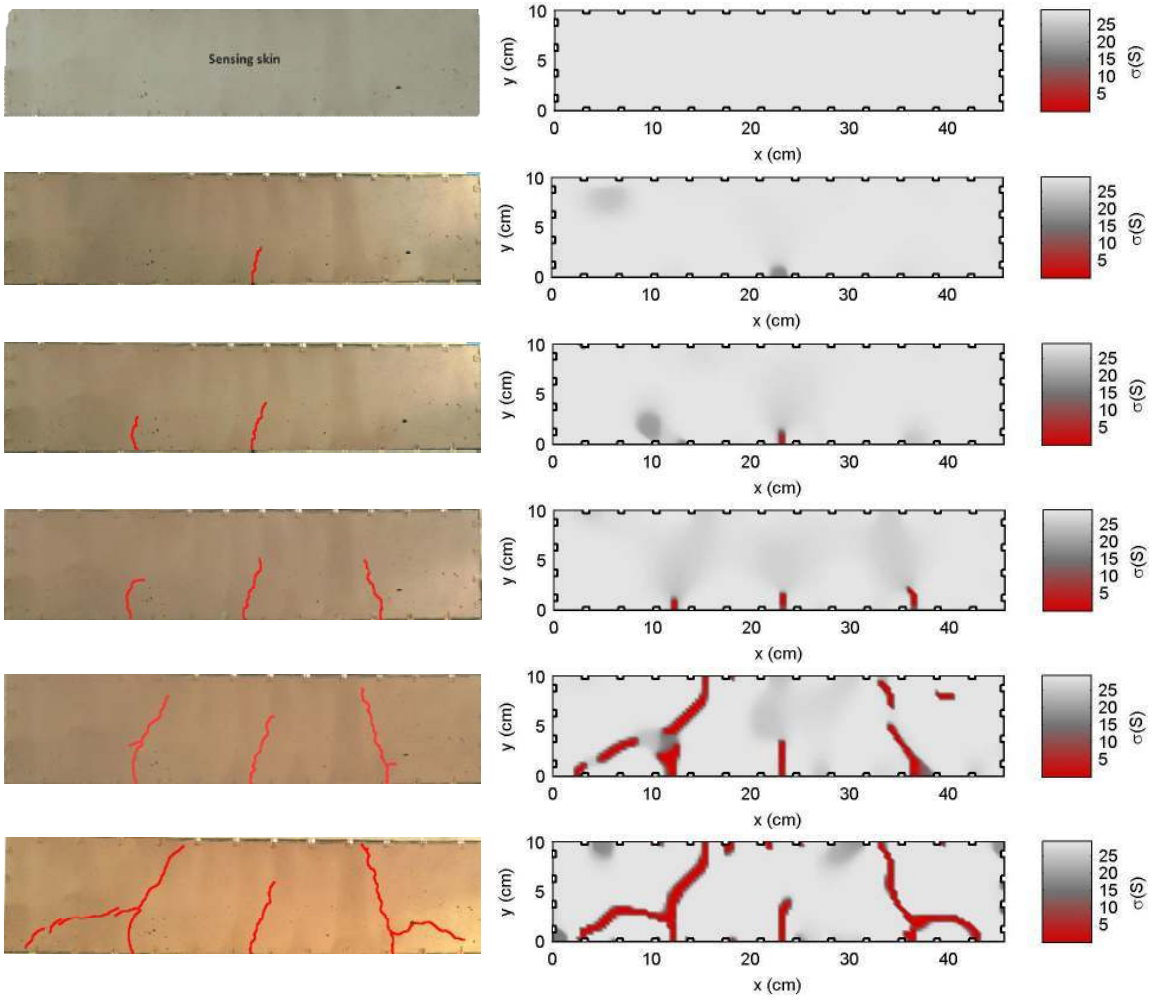

Figure 4: Single layer sensing skin applied on a concrete beam surface; photographs of the sensing skin (left column) and EIT reconstructions of the sensing skin (right column).

5 DETECTION OF CHLORIDES AND CRACKING WITH EIT-BASED MULTI-LAYER SENSING SKIN

5.1 Experiments

An EIT-based sensing skin (such as that in Section 4) monitors phenomena on the substrate surface via imaging local changes in the electrical conductivity of the sensing skin. To detect the presence of chlorides with a sensing skin, its conductivity thus needs to alter under the influence of chlorides. However, since the conductivity of virtually any conductive material changes also if it cracks, it would be very difficult to distinguish between the presence of chlorides and cracking, if only a single layer of sensing skin sensitive to chlorides was used. Therefore, we propose a multi-layer sensing skin where chlorides change the conductivity of one of the layers while the second layer is not affected by the chlorides. If successful, the latter layer reveals the locations of cracks, and enables distinguishing between the chlorides and cracks on the first layer.

Figure 5 shows a schematic image of the multi-layer sensing skin used in this experiment. The three-layers of the sensing skin were applied on the reinforced concrete beam; first a

copper (Cu) layer was painted on the surface of the beam. Next, the Cu layer was covered with the layers of latex and silver (Ag) paint. These materials were chosen based on an another experiment, where the Cu paint was shown to be sensitive to exposure of chlorides, whereas the Ag paint was shown to not be affected by chlorides.

The purpose of the experiment was to test the feasibility of the designed multi-layer sensing skin for detection of chlorides and cracking. Thus, the reinforced concrete beam was first subjected to ingress of chlorides, and subsequently, to cracking by 3-point bending. The specimen was prepared and the experiment was carried out as follows. The details are explained in manuscript [17].

When casting the concrete beam, a section of a PVC pipe with 2.54 cm inner diameter was embedded inside the beam at an angle, forming a reservoir for NaCl solution. The embedded end was positioned approximately at 2.50 cm distance from the beam face on which the sensing skin was applied. The location of the embedded end of the reservoir was approximately under electrode 2 of the Ag layer (Figure 5). The reservoir was filled with saturated NaCl solution, and the solution was let to be absorbed by the concrete from the embedded end of the reservoir for 144 hours. The first sets of EIT measurements were carried out before starting the NaCl exposure, and then after every 24 hours up to 144 hours of NaCl solution ingress. After this, the beam was loaded in a 3-point bending test. A displacement controlled loading with a rate of 0.13 cm/min was applied in a closed-loop universal testing machine, and the vertical displacement in the mid-span of the beam was measured by the testing machine. EIT measurements were carried out at several levels of loading.

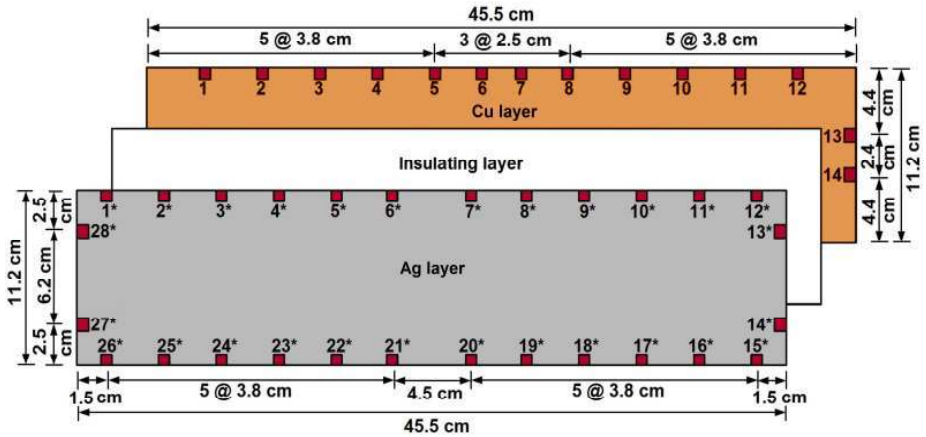

Figure 5: Schematic illustration of the multi-layer sensing skin applied on the surface of a concrete beam.

5.2 Results

The results of the experiment with the multi-layer sensing skin are shown in Figure 6. The left column shows photographs of the sensing skin at times of EIT measurements, and the middle and left column represent the EIT reconstructions of the Ag (crack detection) and Cu (chloride and crack detection) layer, respectively.

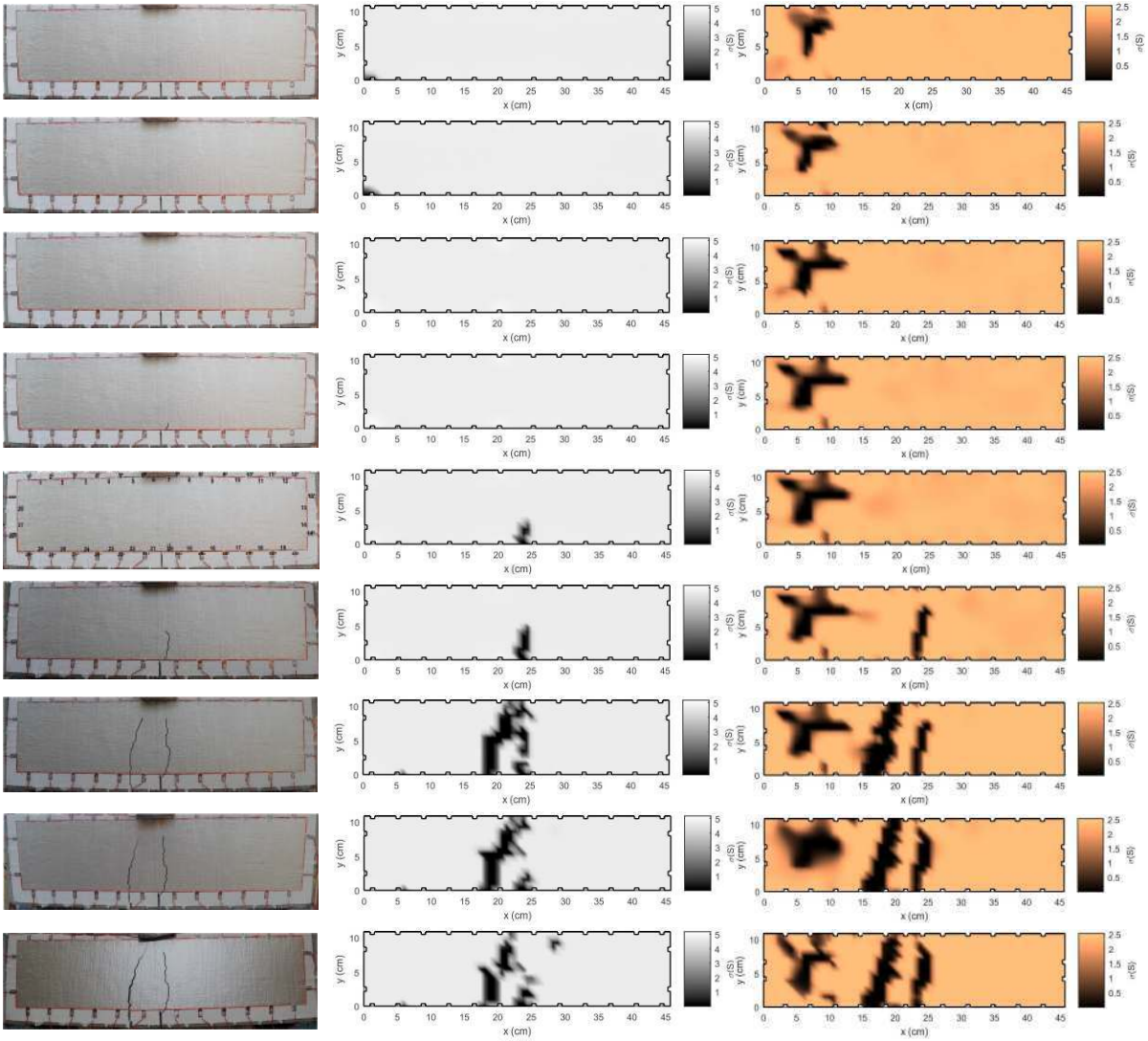

Figure 6: Photographs of the sensing skin at times of EIT measurements (left column), and the corresponding EIT reconstructions of the Ag [crack detection] layer (middle column) and the Cu [chloride and crack detection] layer (right column). The first four lines correspond to times 12, 24, 96 and 144 hours of chloride solutions ingress, and the last five lines correspond to three-point bending at load levels 11.6, 16.9, 27.6, 23.1 and 21.8 kN.

The first four lines in Figure 6 correspond to times 12, 24, 96 and 144 hours of chloride ingress. At these stages, the Ag layer remains practically unaltered. The EIT reconstruction of the Cu layer, on the other hand, shows a spot with significantly reduced conductivity right under electrode 2, i.e., in the location of the embedded end of the reservoir NaCl reservoir. This result indicates that the Cu layer of the sensing skin is able to detect the presence of Chlorides, as expected. The following five lines in Figure 6 correspond to three-point bending at load levels 11.6, 16.9, 27.6, 23.1 and 21.8 kN. In the corresponding reconstructions, both sensing skin layers feature a strong decrease of conductivity roughly in the locations of the cracks shown in the photographs.

In this experiment, the reconstructions of both layers were overall of lower quality than in single-layer sensing skin in Section 4. This was a result of higher noise/mutual interference between electrodes and wires attached to the two layers in the sensing skin. Nevertheless, the series of images in Figure 6 demonstrate the feasibility of the proposed multi-layer sensing skin for the detection of chloride attacks and cracking in concrete structures. The Cu layer of the sensing skin detects the location of the chlorides migrated through the concrete and the cracks induced by the 3-point bending, while the Ag layer detects only the cracks. Despite the inaccuracies in the reconstructions of the Ag layer conductivity, the cracks are clearly visible, and the Ag layer of the sensing skin allows for distinguishing between the chloride damage and cracks in the Cu layer.

5 CONCLUSIONS

In this paper, two applications of EIT in structural health monitoring were considered: imaging unsaturated moisture flows in cement-based materials, and detecting the presence of chlorides and cracking using an EIT-based (single-/multi-layer) sensing skins. The feasibility of EIT for these applications was studied experimentally.

In the moisture flow monitoring experiment, the EIT reconstructions compared well with the neutron radiographs, supporting the applicability of EIT to detect the unsaturated moisture flows in cement-based materials. The results with the sensing skins demonstrate the feasibility of a single-layer sensing skin for detecting cracks, and further, show the potential of a multi-functional multi-layer sensing skin for simultaneously detecting corrosive elements and cracks, and for distinguishing between them.

REFERENCES

[1] A. Neville, Properties of Concrete, 4th edition Wiley, New York, 1996.

[2] R. Gummerson, C. Hall, W. Hoff, R. Hawkes, G. Holland, W. Moore, Unsaturated water flow within porous materials observed by NMR imaging, Nature, **28**, 56–57, 1979.

[3] S. Roels, J. Carmeliet, H. Hens, O. Adan, H. Brocken, R. Cerny, Z. Pavlik, A. Ellis, C. Hall, K. Kumaran, A comparison of different techniques to quantify moisture content profiles in porous building materials, J. Therm. Envel. Build. Sci., **27**, 261–276, 2004.

[4] H. Pleinert, H. Sadouki, F. Wittmann, Determination of moisture distributions in porous building materials by neutron transmission analysis, Mater. Struct, **31**, 218-224, 1998.

[5] W. McCarter, Monitoring the influence of water and ionic ingress on cover zone concrete subjected to repeated absorption, Cement Concr. Aggr., **18**, 55–63, 1996.

[6] W. McCarter, T. Chrisp, G. Starrs, A. Adamson, E. Owens, P. Basheer, S. Nanukuttan, S. Srinivasan, N. Holmes, Developments in performance monitoring of concrete exposed to extreme environments, J. Infrastruct. Syst., **18**, 167–175, 2012.

[7] Du Plooy, R., et al. Electromagnetic non-destructive evaluation techniques for the monitoring of water and chloride ingress into concrete: a comparative study, Materials and Structures, **48**, 369-386, 2015.

[8] M. Hallaji, A. Seppänen, M. Pour-Ghaz, Electrical resistance tomography to monitor

unsaturated moisture flow in cementitious materials. Cement and Concrete Research, **69**, 10-18, 2015.

[9] D. Smyl, M. Hallaji, A. Seppänen, M. Pour-Ghaz, Three-dimensional electrical impedance tomography to monitor unsaturated moisture ingress in cement-based materials. Transport in Porous Media, Submitted.

[10] M. Pour-Ghaz, A. Poursaee, R. Spragg R and J. Weiss, Experimental methods to detect and quantify damage in restrained concrete ring specimens. J. Adv. Concr. Technol. **9**, 251–260, 2011.

[11] T. Schumacher, E. Thostenson. Development of structural carbon nanotube–based sensing composites for concrete structures, Journal of Intelligent Material Systems and Structures, 1045389X13505252, 2013.

[12] T. Hou, K. Loh, J. Lynch () Spatial conductivity mapping of carbon nanotube composite thin films by electrical impedance tomography for sensing applications, Nanotechnology, **18**, 315501, 2007.

[13] K. Loh, T. Hou, J. Lynch, N. Kotov, Carbon nanotube sensing skins for spatial strain and impact damage identification. J. Nondestruct. Eval. **28**: 9–25, 2009.

[14] M. Hallaji, M. Pour-Ghaz, A new sensing skin for qualitative damage detection in concrete elements: Rapid difference imaging with electrical resistance tomography. NDT & E INT **68**, 13–21, 2014.

[15] M. Hallaji, A. Seppänen, M. Pour-Ghaz, Electrical impedance tomography-based sensing skin for quantitative imaging of damage in concrete. Smart Materials and Structures, **23**, 085001, 2014.

[16] A. Seppänen, M. Hallaji, M. Pour-Ghaz, Electrical impedance tomography-based sensing skin for detection of damage in concrete. In: 11th European Conference on Non-Destructive Testing (ECNDT 2014). Prague, Czech Republic, 2014.

[17] A. Seppänen, M. Hallaji, M. Pour-Ghaz, A functionally layered sensing skin for detection of corrosive elements and cracking, Structural Health Monitoring. Submitted, 2016.

[18] W. Daily, A. Ramirez, D. LaBrecque, J. Nitano, Electrical resistivity tomography of vadose water movement, Water. Resour. Res. **28**, 1429–42, 1992.

[19] T. Tidswell, A. Gibson, R.H. Bayford, D.S. Holder, Three-dimensional electrical impedance tomography of human brain activity NeuroImage, **13**, 283–94, 2001

[20] D. Scott, H. McCann (ed) Handbook of Process Imaging for Automatic Control, Boca Raton, FL: CRC Press, 2005

[21] J. Mueller, S. Siltanen, Linear and Nonlinear Inverse Problems with Practical Applications, Philadelphia: SIAM, 2012.